


Article

Influence of Oxygen Ion Migration from Substrates on Photochemical Degradation of $\text{CH}_3\text{NH}_3\text{PbI}_3$ Hybrid Perovskite

Ivan S. Zhidkov ^{1,2,*} , Azat F. Akbulatov ³, Liana N. Inasaridze ³, Andrey I. Kukhareenko ¹, Lyubov A. Frolova ³, Seif O. Cholakh ¹, Chu-Chen Chueh ⁴, Pavel A. Troshin ³ and Ernst Z. Kurmaev ^{1,2}

¹ Institute of Physics and Technology, Ural Federal University, Mira St. 19, 620002 Yekaterinburg, Russia; a.i.kukhareenko@urfu.ru (A.I.K.); s.o.cholakh@urfu.ru (S.O.C.); ernst.kurmaev@gmail.com (E.Z.K.)

² M. N. Mikheev Institute of Metal Physics of Ural Branch of Russian Academy of Sciences, S. Kovalevskoi St. 18, 620108 Yekaterinburg, Russia

³ Institute for Problems of Chemical Physics, The Russian Academy of Sciences (IPCP RAS), Semenov Prospect 1, 141432 Chernogolovka, Russia; qweas89@mail.ru (A.F.A.); liana.inasaridze@gmail.com (L.N.I.); lyubovanatolievna@mail.ru (L.A.F.); troshin2003@inbox.ru (P.A.T.)

⁴ Advanced Research Center for Green Materials Science and Technology, Department of Chemical Engineering, National Taiwan University, Taipei 10617, Taiwan; cchueh@ntu.edu.tw

* Correspondence: i.s.zhidkov@urfu.ru

Abstract: Measurements of XPS survey, core levels (N 1s, O 1s, Pb 4f, I 3d), and valence band (VB) spectra of $\text{CH}_3\text{NH}_3\text{PbI}_3$ (MAPbI₃) hybrid perovskite prepared on different substrates (glass, indium tin oxide (ITO), and TiO_2) aged under different light-soaking conditions at room temperature are presented. The results reveal that the photochemical stability of MAPbI₃ depends on the type of substrate and gradually decreases when glass is replaced by ITO and TiO_2 . Also, the degradation upon exposure to visible light is accompanied by the formation of MAI, PbI_2 , and Pb^0 products as shown by XPS core levels spectra. According to XPS O 1s and VB spectra measurements, this degradation process is superimposed on the partial oxidation of lead atoms in ITO/MAPbI₃ and TiO_2 /MAPbI₃, for which Pb–O bonds are formed due to the diffusion of the oxygen ions from the substrates. This unexpected interaction leads to additional photochemical degradation.

Keywords: hybrid perovskites; XPS; light-induced degradation; oxygen ions; substrates



Citation: Zhidkov, I.S.; Akbulatov, A.F.; Inasaridze, L.N.; Kukhareenko, A.I.; Frolova, L.A.; Cholakh, S.O.; Chueh, C.-C.; Troshin, P.A.; Kurmaev, E.Z. Influence of Oxygen Ion Migration from Substrates on Photochemical Degradation of $\text{CH}_3\text{NH}_3\text{PbI}_3$ Hybrid Perovskite. *Energies* **2021**, *14*, 5062. <https://doi.org/10.3390/en14165062>

Academic Editor: Antonino Laudani

Received: 11 July 2021

Accepted: 13 August 2021

Published: 17 August 2021

Publisher's Note: MDPI stays neutral with regard to jurisdictional claims in published maps and institutional affiliations.



Copyright: © 2021 by the authors. Licensee MDPI, Basel, Switzerland. This article is an open access article distributed under the terms and conditions of the Creative Commons Attribution (CC BY) license (<https://creativecommons.org/licenses/by/4.0/>).

1. Introduction

The possibility of using hybrid perovskites in photovoltaics was demonstrated 10 years ago [1]. Since then, these materials have become the subject of numerous studies and still attract enormous interest due to their excellent optoelectronic properties, low manufacturing costs, tunable bandgaps, and high efficiency [2–5]. These materials can be solution-processed at low temperature and vapor-deposited, realistically holding the promise to reach comparable efficiency as conventional thin-film photovoltaic technologies had. Besides, they can be combined with organic electron or hole transport materials to realize flexible photovoltaic devices. However, the instability of these materials to light, moisture, and temperature has aroused a serious concern that needs to be addressed prior to commercial use. For example, hybrid perovskites were found to decompose when exposure to the ambient atmosphere due to the chemical reactions between themselves and humidity/oxygen in the air [6]. In this regard, various encapsulation technologies have been applied to hybrid perovskite photovoltaic devices to increase their service life [7]. Nevertheless, it should be noted that much less attention is paid to the chemical reactions between lead iodides and oxygen ions diffused from oxide substrates or electron transport layers, which migrate under the influence of light and temperature. This issue is addressed in this article, where the photochemical stability of glass/MAPbI₃, ITO/MAPbI₃, and TiO_2 /MAPbI₃ junctions was systematically studied with the assistance of X-ray photoelectron spectroscopy (XPS).

2. Experimental

Glass slides (ISOLAB objective glass), glass/ITO (5 Ω , Luminescence Technology Corp., New Taipei, Taiwan), and glass/TiO₂ (10 Ω , Luminescence Technology Corp., New Taipei, Taiwan) substrates were sequentially cleaned with toluene and acetone and sonicated in deionized water, acetone, and isopropanol. The 0.5 M MAPbI₃ precursor solutions in dimethylformamide (DMF) were spin-coated on top of the glass, glass/ITO, and glass/TiO₂ substrates at 4000 rpm inside a nitrogen-filled glove box. Toluene (100 μ L) was dropped seven seconds after the start of the spinning thus quenching the precursor and inducing the film crystallization. Spinning was continued for 30 s and then the deposited films were annealed inside a glove box at 100 $^{\circ}$ C for 5 min. The photochemical aging experiments were performed under well-controlled anoxic conditions using specially designed setups integrated into the dedicated MBraun glove box using an LG sulfur plasma lamp as a standard light source, which provides a good approximation of the solar AM1.5G spectrum. The light power at the samples was ~ 70 mW/cm², while the temperature was 45 ± 2 $^{\circ}$ C (enabled by intense fan cooling of the sample stage).

Scanning electron microscopy images were obtained on Zeiss SUPRA 25 equipment (Jena, Germany). The samples were prefixed on a microscope stage inside the glove box to reduce the exposure time in the air down to ~ 1 min. XRD patterns were recorded using a Bruker D8 instrument (Billerica, MA, USA).

XPS was used to measure core level and VB spectra with help of a PHI XPS 5000 VersaProbe spectrometer (ULVAC-Physical Electronics, Chanhassen, MN, USA) with a spherical quartz monochromator and an energy analyzer working in the range of binding energies from 0 to 1500 eV. The energy resolution was $\Delta E \leq 0.5$ eV. The samples were measured at a pressure of 10^{-7} Pa. Finally, XPS spectra were processed using PHI MultiPak 9.9.0.8 software.

3. Results and Discussion

All samples showed notable aging after 300 h of light soaking even under anoxic conditions as could be concluded from the change of their visual appearance: the films become opaque and their color evolved from dark-brown to grayish-yellow. This conclusion was well supported by the scanning electron microscopy (SEM) images shown in Figure 1. Indeed, the typical grainy perovskite film morphology characteristic for the pristine samples changed dramatically after photochemical aging as could be concluded from the formation of poorly interconnected islands most probably represented by the aging products. Interestingly, the morphology of the aged films strongly depends on the type of substrate. Thus, the films grown on soda-lime glass showed the formation of big irregularly shaped islands decorated with tiny spherical or ellipsoidal particles. On the contrary, the perovskite films grown on ITO degraded with the formation of separate grains with uniform shape and 50–60 nm size. Furthermore, using TiO₂ as a substrate promoted the formation of some layered structures.

The evolution of the UV-vis absorption spectra shown in Figure 2 clearly illustrates that glass is the most inert substrate for MAPbI₃ since the photobleaching of the perovskite films occurs at the lowest rate. Furthermore, the absorption profile of the films after 200 h of aging closely resembles that of PbI₂ as could be concluded from the presence of the sharp feature at ~ 500 nm. In contrast, the decomposition of MAPbI₃ films on ITO and TiO₂ goes much faster and the absorption profiles of the films become featureless after 200 h, which is suggesting the predominant formation of the metallic lead rather than PbI₂.

Deeper insight into the chemistry of the light-induced decomposition of MAPbI₃ films deposited on different substrates was gained using X-ray diffraction (XRD). The perovskite films grown on glass showed the predominant formation of PbI₂ with just traces of metallic lead (Figure 3a), which is consistent with the UV-vis spectral data. On the contrary, the intensity of the Pb⁰ peak became comparable or even higher than that of the major PbI₂ signature in the case of the films deposited on TiO₂ and ITO substrates (Figure 3b,c). However, one should keep in mind that the intensity of the peaks may not fully correlate with the actual phase composition of the samples due to e.g., different crystallinity of the

components. Still, the obtained results support the conclusion that the substrate material affects not just the rate of the light-induced decomposition, but also the composition of the formed products.

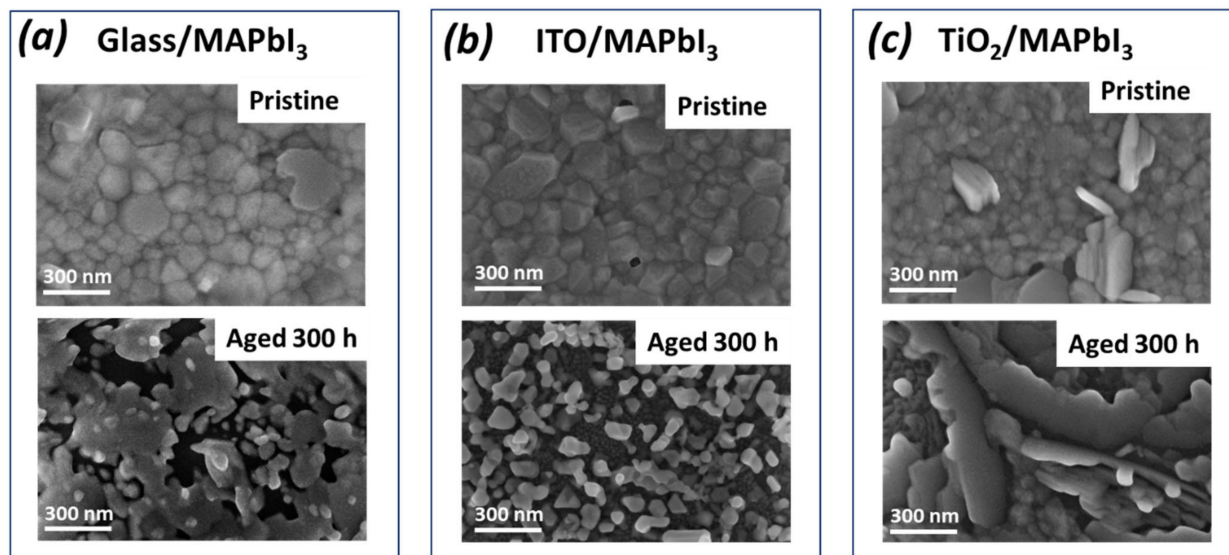


Figure 1. SEM images of MAPbI₃ films grown on (a) glass, (b) ITO, and (c) TiO₂ substrates before and after 300 h of light soaking.

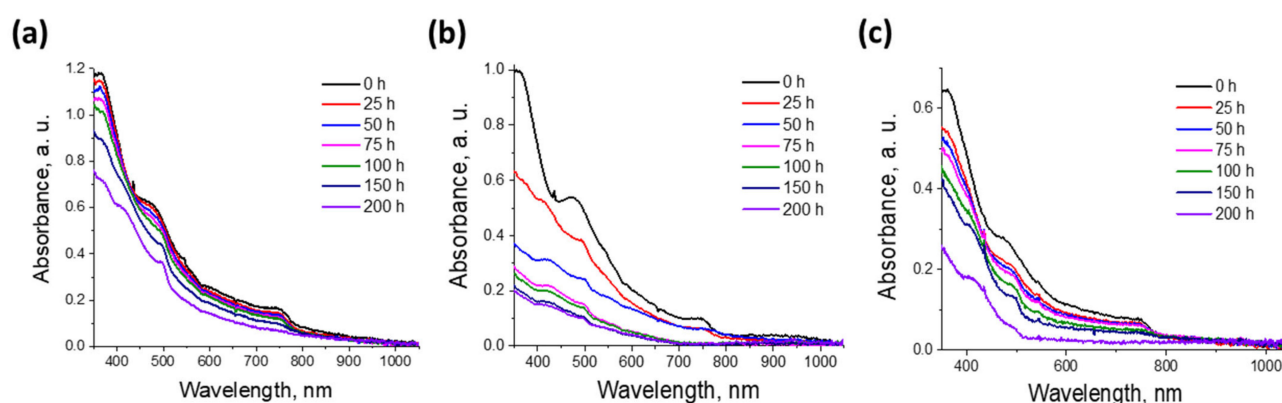


Figure 2. The evolution of the UV-vis spectra of MAPbI₃ films grown on (a) glass, (b) ITO, and (c) TiO₂ substrates upon light soaking under anoxic conditions.

Figure 4 presents the XPS survey spectra of MAPbI₃ before and after light soaking at different aging times. The surface compositions, such as N:Pb and I:Pb ratios, determined from these spectra are summarized in Table 1. Measurements of the surface composition make it possible to determine their changes in the samples under study, while analysis of N:Pb and I:Pb ratios allow us to trace the photochemical degradation of MAPbI₃ depending on the exposure time to visible light. As can be seen in the sample of glass/MAPbI₃, the N:Pb ratio exhibits a moderate decrease from 0.71 to 0.36 as the aging time gradually increases from 25 to 100 h, which indicates the slow, partial decomposition of the organic cation. Only at a 200-h exposure, the N 1s signal ceases to be recorded due to the complete evaporation of nitrogen species. Notably, the I:Pb ratio of MAPbI₃ does not exhibit a significant change (within 2.75–1.95) with the light-soaking time.

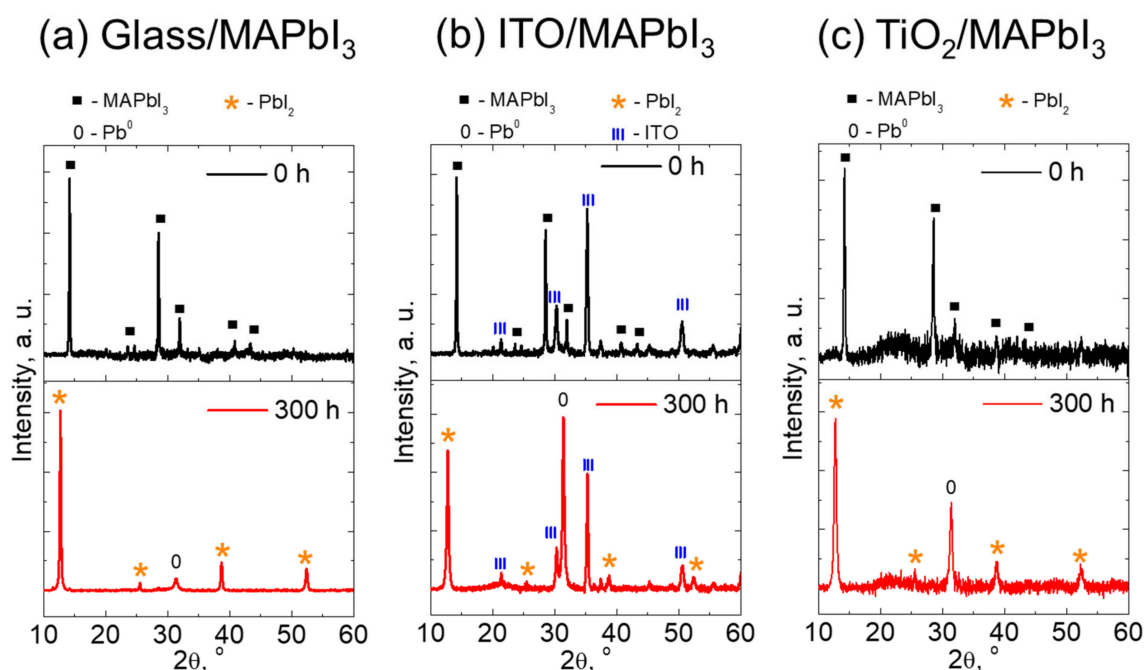


Figure 3. XRD patterns of MAPbI₃ films grown on (a) glass, (b) ITO, and (c) TiO₂ substrates before and after 300 h of light soaking.

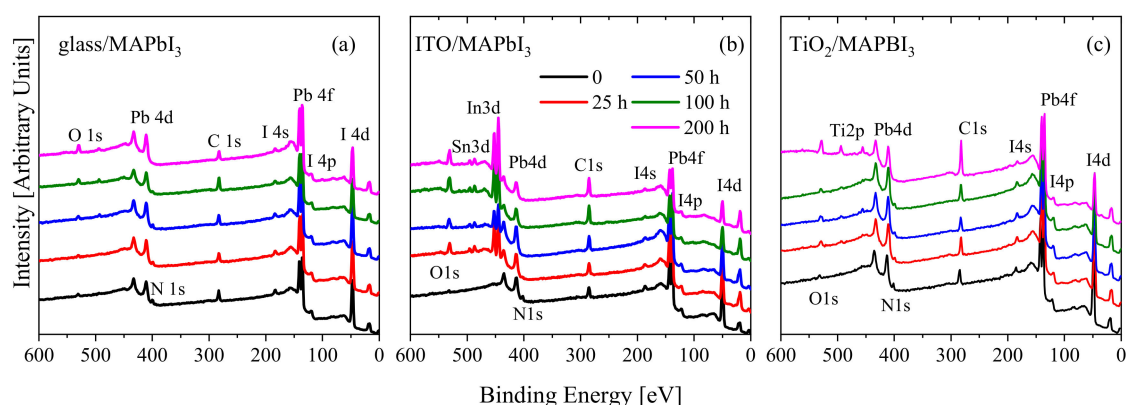
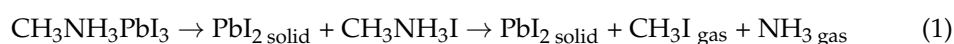


Figure 4. XPS survey spectra of light-soaked MAPbI₃ hybrid perovskites prepared on: (a) glass, (b) ITO, and (c) TiO₂ substrates.

Table 1. Surface composition of the as-prepared and light-irradiated CH₃NH₃PbI₃ samples (at. %).

Sample	C	O	N	I	Pb	Sn	In	Na	Si	Ti	I:Pb	N:Pb
Glass/MAPbI₃	39.3	3.5	9.1	35.3	12.8	-	-	-	-	-	2.75	0.71
Photo, 25 h	41	4	7	34.1	13.9	-	-	-	-	-	2.45	0.50
Photo, 50 h	38.8	5.2	6.1	33.6	13.9	-	-	2.4	-	-	2.41	0.43
Photo, 100 h	45.7	9	4	25	10.9	-	-	3.6	1.8	-	2.29	0.36
Photo, 200 h	37.5	15.5	-	25.3	13	-	-	5.2	3.5	-	1.94	-
ITO/MAPbI₃	44.9	2.3	8.7	32.2	11.9	-	-	-	-	-	2.70	0.73
Photo, 25 h	39.3	17.2	1.9	21.1	10	1.1	9.4	-	-	-	2.11	0.19
Photo, 50 h	46.2	16	-	19.3	11.6	0.9	6	-	-	-	1.66	-
Photo, 100 h	48.1	21.5	0.8	9.9	6	1	10.8	-	1.9	-	1.65	0.13
Photo, 200 h	49.9	20.5	-	10.2	6.5	1.1	11.8	-	-	-	1.56	-
TiO₂/MAPbI₃	43.5	2.3	10.2	32.7	11.3	-	-	-	-	-	2.89	0.90
Photo, 25 h	32.7	25.8	1.6	20	10.8	0.5	0.1	-	-	8.5	1.85	0.14
Photo, 50 h	32.9	27.2	2.1	17.7	9.8	0.7	0.2	-	-	9.4	1.80	0.21
Photo, 100 h	41.6	28.2	1.5	11.2	6.5	1	0.2	-	-	9.8	1.72	0.23
Photo, 200 h	45.8	28.9	1.4	7.1	5.7	0.4	0.2	-	-	10.5	1.24	0.24

Surprisingly, much more significant changes in these ratios depending on aging time (25–200 h) were observed for the other two systems. For ITO/MAPbI₃, the N:Nb ratio decreases from 0.73 to 0.13, and the I:Pb ratio decreased from 2.70 to 1.56 while, for TiO₂/MAPbI₃, the N:Nb ratio is reduced from 0.90 to 0.24 and the I:Pb ratio is reduced from 2.89 to 1.24. As shown earlier [8–10], a decrease in the N:Nb ratio indicates the decomposition of the organic cation, whereas reduction of I:Pb suggests the formation of PbI₂, a product of decomposition of hybrid perovskites. On the one hand, these conclusions fit well into the degradation scheme as proposed in [11,12]:



On the other hand, glass/MAPbI₃ turned out to be the most resistant to visible light irradiation as compared to ITO/MAPbI₃ and TiO₂/MAPbI₃.

Measurements of XPS N 1s, Pb 4d, and I 3d core-level spectra with a high energy resolution are capable to verify the validity of these conclusions. Relevant data are given in Figures 5–7. As first shown in Figure 5, the relative intensities of XPS N 1s spectra normalized to XPS Pb 4d-intensity show that some dependence on the aging time is still visible for the glass/MAPbI₃ system; however, it is not actually observed for the other two ones, for which the N 1s/Pb 4d relative intensity drops sharply starting from 50 h.

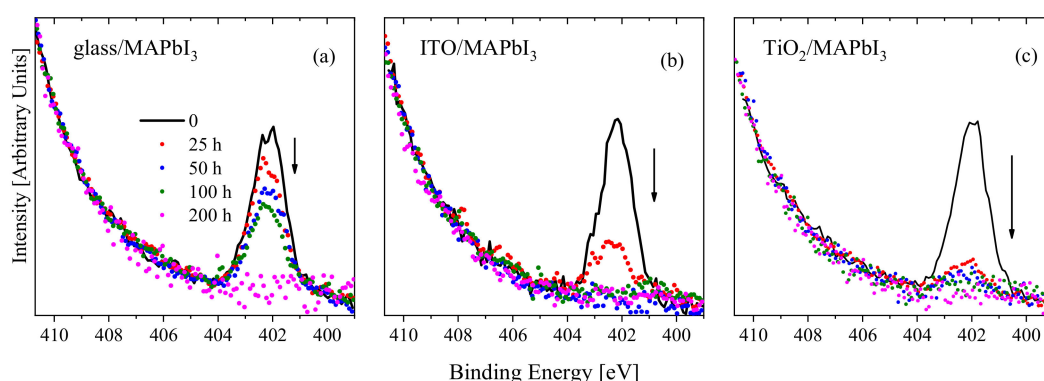


Figure 5. XPS N 1s spectra normalized on Pb 5d-line of light-soaked MAPbI₃ hybrid perovskites prepared on different substrates: (a) glass, (b) ITO, and (c) TiO₂ substrates.

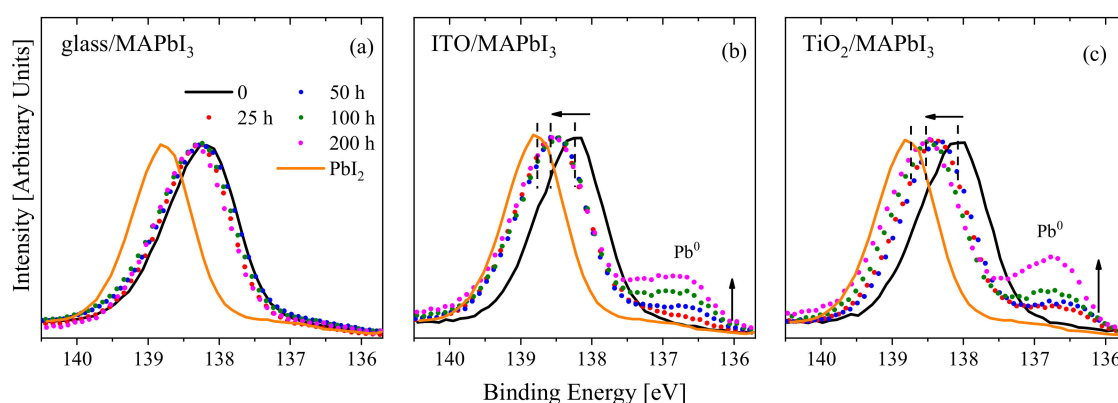


Figure 6. XPS Pb 4f_{7/2} spectra of light-soaked MAPbI₃ hybrid perovskites prepared on different substrates: (a) glass, (b) ITO, and (c) TiO₂ substrates.

Figures 6 and 7 respectively present the dependence of the measured XPS Pb 4f and I 3d spectra of these three systems on the aging time and compare them with the spectra of PbI₂ compound that is the final product of photochemical degradation of MAPbI₃ hybrid perovskite. As shown, the energy position of XPS Pb 4f and I 3d spectra of PbI₂ is a

benchmark, the proximity to which makes it possible to judge the degree of photochemical degradation.

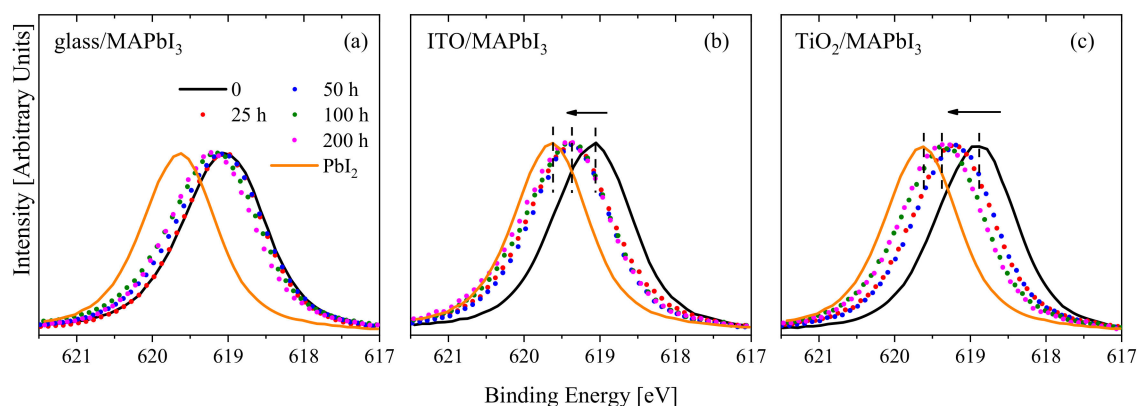


Figure 7. XPS I 3d_{5/2} spectra of light-soaked MAPbI₃ hybrid perovskites prepared on different substrates: (a) glass, (b) ITO, and (c) TiO₂ substrates.

Notably, another benchmark is the energy position of the original (unirradiated) perovskites. The energy position of XPS Pb 4f and I 3d spectra measured under different aging times between these two reference points allows us to judge the degree of photochemical decomposition of the investigated materials. To better analyze XPS Pb 4f spectra, we have one more reference, which is the energy position of the pure lead metal (Pb⁰). According to the degradation mechanism proposed in [13], further irradiation of PbI₂ (one of the primary degradation products) will lead to its decay into MAI and Pb⁰. Considering all of these factors, it is possible to analyze the experimental data presented in Figures 6 and 7 as follows. According to these data, XPS Pb 4f and I 3d spectra of irradiated glass/MAPbI₃ system are close in energy position to initial materials, which indicates their superior photochemical stability. On the contrary, for ITO/MAPbI₃ and TiO₂/MAPbI₃ systems, a high-energy shift of XPS Pb 4f and I 3d spectra with the aging time is observed, and this effect is much more pronounced for the TiO₂/MAPbI₃ system. In addition, for both systems, Pb⁰ phase loss is also observed in XPS Pb 4f spectra and the relative intensity of this contribution is increasing with exposure time. This means that further decomposition of PbI₂ occurs in this case. Thus, the above results of high-energy resolved XPS N 1s, Pb 4f, and I 3d spectra leads to the same conclusion that we made from measurements of XPS survey spectra. That is, among these three studied systems, the glass/MAPbI₃ system is the most resistant to visible light irradiation, then ITO/MAPbI₃ and TiO₂/MAPbI₃, respectively, go in terms of the degree of stability loss.

We then try to understand the reason for the difference in photochemical stability of the same MAPbI₃ perovskite prepared on three different substrates. Oxygen is a common component for all three substrates used; therefore, first of all, the effect of irradiation on the state of oxygen in these systems is of interest. For this purpose, measurements of XPS O 1s spectra were carried out and the results are presented in Figure 8. As in the previous cases, the chemical state of the investigated element is herein determined by the energy position of the XPS spectrum. There are two starting points here: the chemical position of adsorbed and chemically bound oxygen (lattice oxygen). According to Ref. [14], the energy position of hydrogenated oxygen (O–H) is fixed in the range of 531.5–532.5 eV, and oxygen chemically bonded to the metal (O–Me) fluctuates in the range of 529–530.5 eV [15]. Hence, the data shown in Figure 5 allow us to conclude that, for the glass/MAPbI₃ system, the presence of only adsorbed oxygen on the sample surface is fixed. However, for ITO/MAPbI₃ system, the chemically bound oxygen already appears on the surface of the sample, and its concentration increases with the aging time. For TiO₂/MAPbI₃ system, the contribution of chemically bound oxygen is already decisive on the surface of the sample.

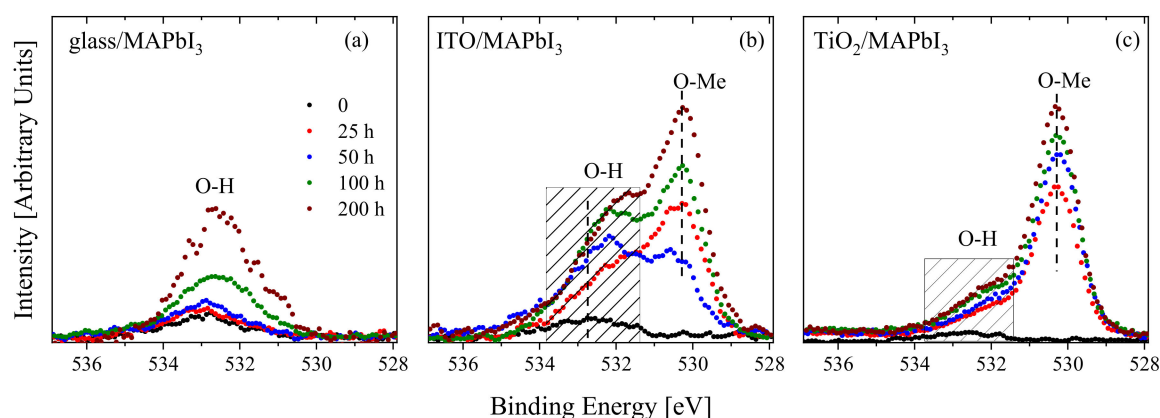


Figure 8. XPS Pb O 1s spectra of light-soaked MAPbI₃ hybrid perovskites prepared on different substrates: (a) glass, (b) ITO, and (c) TiO₂ substrates.

It should be noted that the most suitable metal for oxidation in these systems is lead and the next stage of our study is to obtain experimental data to support this judgment. For this purpose, we measured XPS valence band (VB) spectra of as-prepared (fresh) and light-soaked (at 200 h) glass/MAPbI₃, ITO/MAPbI₃, and TiO₂/MAPbI₃ samples as shown in Figure 9. Identification of XPS VB Pb 6s and I 5p subbands in this figure is in accordance with the DFT calculation of the electronic structure of MAPbI₃ performed in Ref. [9]. First of all, we note the appearance of a new low-energy feature at the energy range of 6–9 eV in XPS VB spectra of ITO/MAPbI₃ and TiO₂/MAPbI₃, where, according to the DFT calculation of MAPbI₃ [9], Pb 6s states are concentrated, while this feature is absent in the spectrum of glass/MAPbI₃ system. The origin of these changes becomes clear from a comparison of these XPS spectra with the calculation result of the total density of states of lead oxide [16], which is also shown in Figure 9. The low-energy subband of the calculated spectrum located at 6–8 eV, which is the result of the hybridization of Pb 6s–O 2p states, correlates well in energy with this new feature of XPS VB spectra. Thus, from the correspondence between the experimental and calculated data, it can be concluded that lead atoms in ITO/MAPbI₃ and TiO₂/MAPbI₃ systems chemically interact with oxygen atoms. It should be noted that, in XPS VB spectra, an increased contribution of Pb 6s–O 2p states is observed for TiO₂/MAPbI₃ system compared to the ITO/MAPbI₃ system, which is in good agreement with the change in the contributions of chemically bound oxygen (O–Me) to the XPS O 1s spectra (Figure 8).

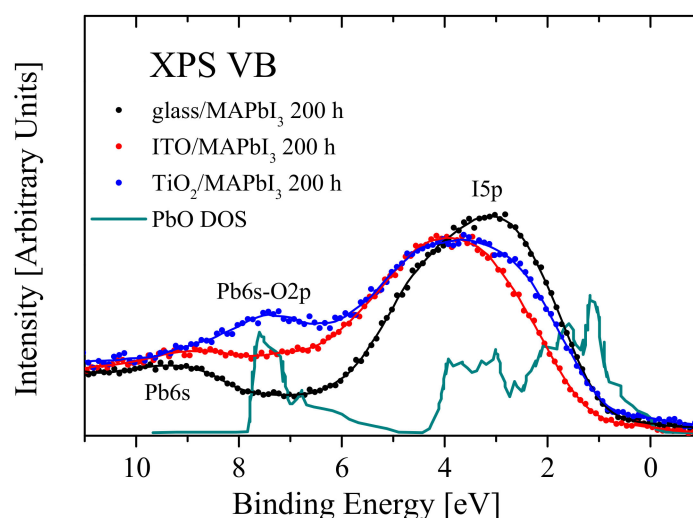


Figure 9. XPS VB spectra of light-soaked MAPbI₃ hybrid perovskites prepared on different substrates as indicated.

4. Conclusions

Measurements of XPS spectra have shown that, under irradiation of MAPbI₃ hybrid perovskites with visible light (25–200 h), their partial photochemical degradation occurs and it is more pronounced on ITO and TiO₂ substrates than on a glass substrate. This degradation is accompanied by the appearance of MAI, PbI₂, and Pb⁰ decay products as evidenced by XPS N 1s, Pb 4f, and I 3d spectra. At the same time, the oxygen ions migrate from the substrates to perovskite and interact with the decomposition products to result in the formation of OH-containing and lead-oxygen species as concluded from the XPS O 1s and VB spectra. The oxidation of the perovskite material by the oxygen from the substrate induces additional photochemical degradation, and, therefore, both ITO/MAPbI₃ and TiO₂/MAPbI₃ junctions are found to be less stable to light soaking than glass/MAPbI₃ system.

Author Contributions: Conceptualization, E.Z.K. and P.A.T.; methodology, I.S.Z.; formal analysis, I.S.Z. and E.Z.K.; investigation, I.S.Z., A.F.A., L.N.I., A.I.K., S.O.C. and L.A.F.; resources, P.A.T., A.F.A. and S.O.C.; data curation, E.Z.K.; writing—original draft preparation, E.Z.K.; writing—review and editing, I.S.Z., P.A.T. and C.-C.C.; supervision, E.Z.K., P.A.T. and C.-C.C.; funding acquisition, S.O.C., I.S.Z., E.Z.K., P.A.T. and C.-C.C. All authors have read and agreed to the published version of the manuscript.

Funding: The sample preparation, aging experiments, UV-vis, XRD, and SEM characterization were supported by Russian Science Foundation (project No. 19-73-30020). The XPS measurements were supported by the Ministry of Education and Science of the Russian Federation (project FEUZ-2020-0060), Theme ‘Electron’, no. AAAA-A18-118020190098-5 and Russian Foundation for Basic Research (projects No. 21-52-52002/21 and 20-42-660003). C.-C.C. acknowledges the financial support from the Ministry of Science and Technology in Taiwan (MOST 110-2923-E-002-007-MY3) and the Top University Project from National Taiwan University (110L7836 and 110L7726).

Institutional Review Board Statement: Not applicable.

Informed Consent Statement: Not applicable.

Data Availability Statement: All data supporting the conclusions provided in the article.

Conflicts of Interest: The authors declare no conflict of interest.

References

1. Kojima, A.; Teshima, K.; Shirai, Y.; Miyasaka, T. Organometal halide perovskites as visible-light sensitizers for photovoltaic cells. *J. Am. Chem. Soc.* **2009**, *131*, 6050–6051. [[CrossRef](#)] [[PubMed](#)]
2. Grätzel, M. The light and shade of perovskite solar cells. *Nat. Mater.* **2014**, *13*, 838–842. [[CrossRef](#)]
3. Antonietta Loi, M.; Hummelen, J.C. Perovskites under the Sun. *Nat. Mater.* **2013**, *12*, 1087–1089. [[CrossRef](#)] [[PubMed](#)]
4. Shi, Z.; Jayatissa, A. Perovskites-Based Solar Cells: A Review of Recent Progress, Materials and Processing Methods. *Materials* **2018**, *11*, 729. [[CrossRef](#)] [[PubMed](#)]
5. Grätzel, M. The Rise of Highly Efficient and Stable Perovskite Solar Cells. *Acc. Chem. Res.* **2017**, *50*, 487–491. [[CrossRef](#)] [[PubMed](#)]
6. Cheng, Y.; So, F.; Tsang, S.-W. Progress in air-processed perovskite solar cells: From crystallization to photovoltaic performance. *Mater. Horiz.* **2019**, *6*, 1611–1624. [[CrossRef](#)]
7. Fu, Z.; Xu, M.; Sheng, Y.; Yan, Z.; Meng, J.; Tong, C.; Li, D.; Wan, Z.; Ming, Y.; Mei, A.; et al. Encapsulation of Printable Mesoscopic Perovskite Solar Cells Enables High Temperature and Long-Term Outdoor Stability. *Adv. Funct. Mater.* **2019**, *29*, 1809129. [[CrossRef](#)]
8. Zhidkov, I.S.; Boukhvalov, D.W.; Akbulatov, A.F.; Frolova, L.A.; Finkelstein, L.D.; Kukhareno, A.I.; Cholakh, S.O.; Chueh, C.-C.; Troshin, P.A.; Kurmaev, E.Z. XPS spectra as a tool for studying photochemical and thermal degradation in APbX₃ hybrid halide perovskites. *Nano Energy* **2020**, *79*, 105421. [[CrossRef](#)]
9. Zhidkov, I.S.; Poteryaev, A.I.; Kukhareno, A.I.; Finkelstein, L.D.; Cholakh, S.O.; Akbulatov, A.F.; Troshin, P.A.; Chueh, C.-C.; Kurmaev, E.Z. XPS evidence of degradation mechanism in CH₃NH₃PbI₃ hybrid perovskite. *J. Phys. Condens. Matter* **2020**, *32*, 095501. [[CrossRef](#)] [[PubMed](#)]
10. Zhidkov, I.S.; Boukhvalov, D.W.; Kukhareno, A.I.; Finkelstein, L.D.; Cholakh, S.O.; Akbulatov, A.F.; Juarez-Perez, E.J.; Troshin, P.A.; Kurmaev, E.Z. Influence of Ion Migration from ITO and SiO₂ Substrates on Photo and Thermal Stability of CH₃NH₃SnI₃ Hybrid Perovskite. *J. Phys. Chem. C* **2020**, *124*, 14928–14934. [[CrossRef](#)]
11. Juarez-Perez, E.J.; Hawash, Z.; Raga, S.R.; Ono, L.K.; Qi, Y. Thermal degradation of CH₃NH₃PbI₃ perovskite into NH₃ and CH₃I gases observed by coupled thermogravimetry–mass spectrometry analysis. *Energy Environ. Sci.* **2016**, *9*, 3406–3410. [[CrossRef](#)]

12. Juarez-Perez, E.J.; Ono, L.K.; Uriarte, I.; Cocinero, E.J.; Qi, Y. Degradation Mechanism and Relative Stability of Methylammonium Halide Based Perovskites Analyzed on the Basis of Acid–Base Theory. *ACS Appl. Mater. Interfaces* **2019**, *11*, 12586–12593. [[CrossRef](#)] [[PubMed](#)]
13. Alberti, A.; Bongiorno, C.; Smecca, E.; Deretzis, I.; La Magna, A.; Spinella, C. Pb clustering and PbI₂ nanofragmentation during methylammonium lead iodide perovskite degradation. *Nat. Commun.* **2019**, *10*, 2196. [[CrossRef](#)] [[PubMed](#)]
14. Casalongue, H.S.; Kaya, S.; Viswanathan, V.; Miller, D.J.; Friebe, D.; Hansen, H.A.; Nørskov, J.K.; Nilsson, A.; Ogasawara, H. Direct observation of the oxygenated species during oxygen reduction on a platinum fuel cell cathode. *Nat. Commun.* **2013**, *4*, 2817. [[CrossRef](#)]
15. Moulder, J.F.; Stickle, W.F.; Sobol, P.E.; Bomben, K.D. *Handbook of X-ray Photoelectron Spectroscopy*; Chastain, J., King, R.C.J., Eds.; ULVAK-PHI Inc.: Chanhassen, MN, USA, 1995.
16. Payne, D.J.; Egdel, R.G.; Law, D.S.L.; Glans, P.-A.; Learmonth, T.; Smith, K.E.; Guo, J.; Walsh, A.; Watson, G.W. Experimental and theoretical study of the electronic structures of α -PbO and β -PbO₂. *J. Mater. Chem.* **2007**, *17*, 267–277. [[CrossRef](#)]